

Perceptually Uniform Color Maps for the Disk, Sphere, and Ball

William C. Lenthe and Marc De Graef

Abstract—The use of color to represent multi-dimensional scientific data is ubiquitous. Poorly designed color maps can have uneven perceptual contrast over their range, but recent work has developed design principles for creating high quality color maps for scalars. Our work extends these design guidelines to develop perceptually uniform bicone color maps: HSL-like color spaces that are perceptually uniform in both hue and lightness for any chroma. These color spaces are leveraged to create improved color maps for the disk, the sphere, and the ball.

Index Terms—Psudeocolor, Color, Colormaps, Perception.

1 INTRODUCTION

MULTICOMPONENT psuedocolor maps are widely used to visualize 2D, unit 3D, and 3D vector fields, e.g. phase and magnitude, IPF (inverse pole figure) coloring, and orientation coloring [1]–[3]. These spaces require color maps for the disk, sphere, and ball, respectively. High quality color maps should have uniform perceptual contrast across their entire domain and be free of features [4]. Poor color maps can create artifacts and obscure real features in the underlying data, potentially leading to misinterpretations [5], [6]. Most vector color maps are qualitatively designed to offer a combination of aesthetic appeal and ease of implementation with no clear standards underlying their creation.

Pseudocolor maps are parametric functions in 3D color space [7]. Most electronic displays require colors to be specified in an RGB (red, green, blue) color space [8], with a simple derived grayscale pseudocolor map for a scalar parameter t expressed as follows:

$$t \mapsto (r, g, b) = \left(\frac{t - t_{\min}}{t_{\max} - t_{\min}}, \frac{t - t_{\min}}{t_{\max} - t_{\min}}, \frac{t - t_{\min}}{t_{\max} - t_{\min}} \right) \quad (1)$$

where t_{\min} and t_{\max} are the values mapped to the lower and upper limits of the color map (black and white for a grayscale map). Generally t_{\min} and t_{\max} are the extrema of the values being colored, remapping t to $[0, 1]$, but arbitrary values are possible e.g. to prevent outliers from reducing contrast or maintaining consistent coloring across a series of images [9]. Parameters falling outside of $[0, 1]$ after remapping must be handled, typically by either designating colors for over and under value or clamping [10].

Since HSL (hue, saturation, lightness) and HSV (hue, saturation, value) are cylindrical reparameterizations of RGB space that are more closely aligned with human perception of color [11], [12], they are a common choice for color map

generation, with the same grayscale pseudocolor map being more intuitively expressed as:

$$t \mapsto (h, s, l/v) = \left(0, 0, \frac{t - t_{\min}}{t_{\max} - t_{\min}} \right) \quad (2)$$

Cylindrical and (bi-)conic color spaces are natural choices for pseudocoloring the unit disk, encoding phase and magnitude simultaneously. Using polar coordinates (r, θ) , the most common HSL/HSV choices are a white or black center with maximum chroma at the perimeter:

$$(r, \theta)_w \mapsto (h, s, l) = \left(\frac{\theta}{2\pi} \bmod 1, 1, 1 - \frac{r}{2r_{\max}} \right) \quad (3)$$

$$(r, \theta)_k \mapsto (h, s, l) = \left(\frac{\theta}{2\pi} \bmod 1, 1, \frac{r}{2r_{\max}} \right) \quad (4)$$

$$(r, \theta)_w \mapsto (h, s, v) = \left(\frac{\theta}{2\pi} \bmod 1, \frac{r}{r_{\max}}, 1 \right) \quad (5)$$

$$(r, \theta)_k \mapsto (h, s, v) = \left(\frac{\theta}{2\pi} \bmod 1, 1, \frac{r}{r_{\max}} \right) \quad (6)$$

with w and k subscripts denoting a white and black center respectively. Pseudocoloring for the unit sphere is achieved by first mapping each hemisphere to a disk, typically with a white north pole and black south pole [13]. Although they are widely used, these mappings have visual discontinuities (appearing as brighter or darker radial lines of particular colors) as shown in figure , making them poor color maps. Applying non-linear correction factors to the color map parameterization can reduce the sharpness of these false features [13], but does not improve perceptual contrast uniformity.

CIE (Commission Internationale de l’Éclairage) LAB (L^* , a^* , b^*) and LUV (L^* , u^* , v^*) are color spaces designed to be perceptually uniform in each component [11], making them a more robust space for color map generation. LUV is preferred in this work since it is designed for additive mixtures of light [14], making it more suitable for data visualization on electronic displays. Previous efforts to produce scalar color maps using Euclidean distance in LAB and LUV color spaces have generally been unsuccessful with bi-variate color maps presenting additional challenges

• W.C. Lenthe and M. De Graef are with the Department of Materials Science and Engineering, Carnegie Mellon University, Pittsburgh, PA, 15213.

E-mail: wlenthe@andrew.cmu.edu

E-mail: mdg@andrew.cmu.edu

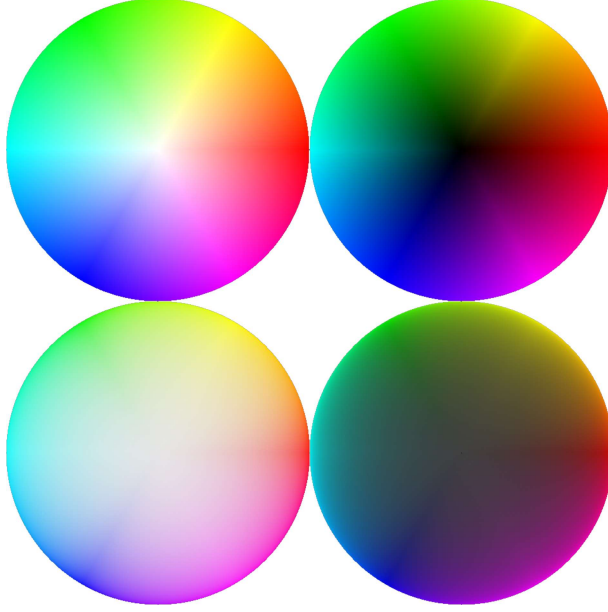


Fig. 1. HSL and HSV based pseudocolor maps of the unit disk are typically white or black at the center with maximum chroma at the perimeter. A white center (top left) is generated by $(r, \theta) \mapsto (h, s, l) = (\theta, 1, 1 - \frac{r}{2})$ and a black center (top right) by $(r, \theta) \mapsto (h, s, l) = (\theta, 1, \frac{r}{2})$. Applying nonlinear scaling to both hue and lightness [13] softens discontinuities but does not eliminate them (bottom left and right).

[15]–[17]. Recent work has demonstrated that a constant lightness (L^*) gradient is most important for high frequency perceptual sensitivity and scalar color maps generated with a constant lightness gradient provide high perceptual uniformity [4]. A constant lightness gradient spline enabled generation of high quality color maps and a sinusoidal ramp was proposed as a test signal for visual evaluation [4]. The test signal is rendered for two scalar color maps:

$$t \mapsto (L^*, u^*, v^*) = \left(\frac{t - t_{\min}}{t_{\max} - t_{\min}}, 0, 0 \right) \quad (7)$$

$$t \mapsto (h^*, s^*, l^*) = \left(\frac{t - t_{\min}}{t_{\max} - t_{\min}}, 1, \frac{1}{2} \right) \quad (8)$$

in figure , demonstrating both the quality of constant lightness gradient color maps and the nonuniformity of hue based color maps; the sinusoidal signal should be equally visible in all regions of the color map in order to have a perceptually uniform map.

The remainder of this paper will detail the extension of perceptually uniform color maps to cylindrical parameterizations suitable for coloring the disk, the sphere, and the ball. Design goals are quantitatively enumerated and a procedure for satisfying them is developed. The procedure is used to construct two reference perceptually uniform cylindrical color spaces. Handling of inversion symmetry within the design constraints is addressed. Finally, the new color spaces are applied to example datasets, demonstrating improvements over existing two parameter color maps.

2 DESIGN GUIDELINES FOR PERCEPTUALLY UNIFORM CYLINDRICAL COLOR SPACES

The simplest approach to generate a perceptually uniform HSL-like color space is to construct a bicone in LUV space

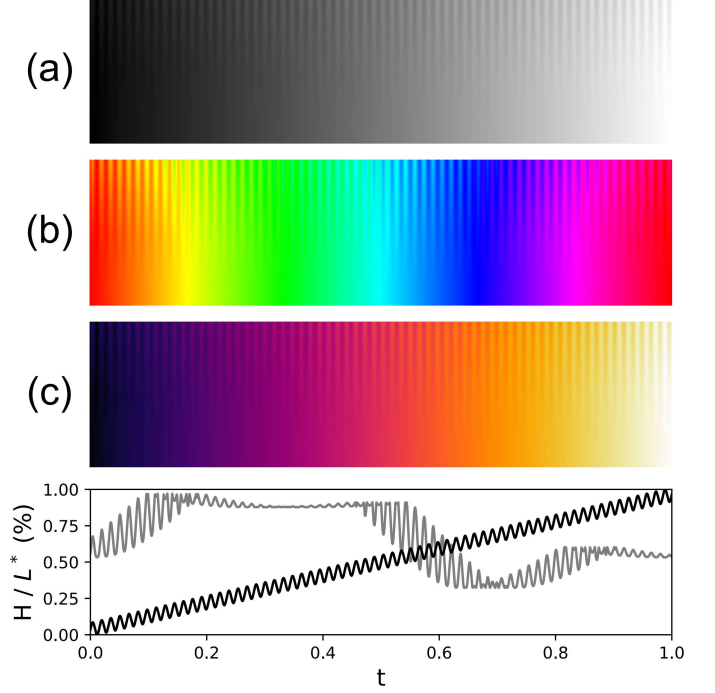


Fig. 2. A sinusoidal ramp (bottom, black) is used as a test signal for evaluating color maps [4]. Color map images have a decreasing amplitude with a flat ramp at the bottom. High quality maps should have uniform sinusoid intensity and be featureless at the bottom. A constant lightness color map (a, equation 7) satisfies both while a hue based color map (b, equation 8) satisfies neither. A high quality pseudocolor map is achieved through a spline with equal lightness spaced control points in LUV space (c). The lightness of the hue based map is plotted in gray with perceptual flat spots near green, blue, and magenta corresponding to regions of low lightness gradient magnitude.

with tips at black and white [18]. This method is straightforward but has two major disadvantages as shown in figure 2: limited chromaticity due to RGB gamut constraints and minimal hue contrast since $\frac{\partial L^*}{\partial \text{hue}} = 0$.

Designing a perceptually uniform HSL-like space, $\text{HSL}_U(h^*, s^*, l^*)$, requires optimization of several competing constraints with chromaticity ($\sqrt{u^{*2} + v^{*2}}$) denoted c^* :

- 1) Grayscale when fully unsaturated: $c^*|_{(h^*, 0, l^*)} = 0$
- 2) Grayscale at lightness endpoints: $c^*|_{(h^*, s^*, 0)} = c^*|_{(h^*, s^*, 1)} = 0$
- 3) Maximum chromaticity at lightness midpoint: $\frac{\partial c^*}{\partial l^*}|_{l^*=\frac{1}{2}} = 0$
- 4) Free from visual discontinuities: $L^*, u^*, v^*(h^*, s^*, l^*) \rightarrow C^1$
- 5) Stay within the RGB gamut: $\text{HSL}_U \subset \text{RGB}$
- 6) Maximize gamut volume: maximize $\int_{h^*, l^*, s^*} \delta L^* \delta u^* \delta v^*$
- 7) Maximize hue contrast: maximize $\Delta_h = \int_{h^*, l^*} \left| \frac{\partial L^*}{\partial h^*} \right|$
- 8) Maximize lightness contrast: maximize $\Delta_l = \int_{h^*, l^*} \left| \frac{\partial L^*}{\partial l^*} \right|$
- 9) Maximize hue perceptual uniformity: minimize $\int_{h^*, l^*} \left| \bar{\Delta}_h - \frac{\partial L^*}{\partial h^*} \right|$
- 10) Maximize lightness perceptual uniformity: minimize $\int_{h^*, l^*} \left| \bar{\Delta}_l - \frac{\partial L^*}{\partial l^*} \right|$
- 11) Evenly distribute contrast between light and dark

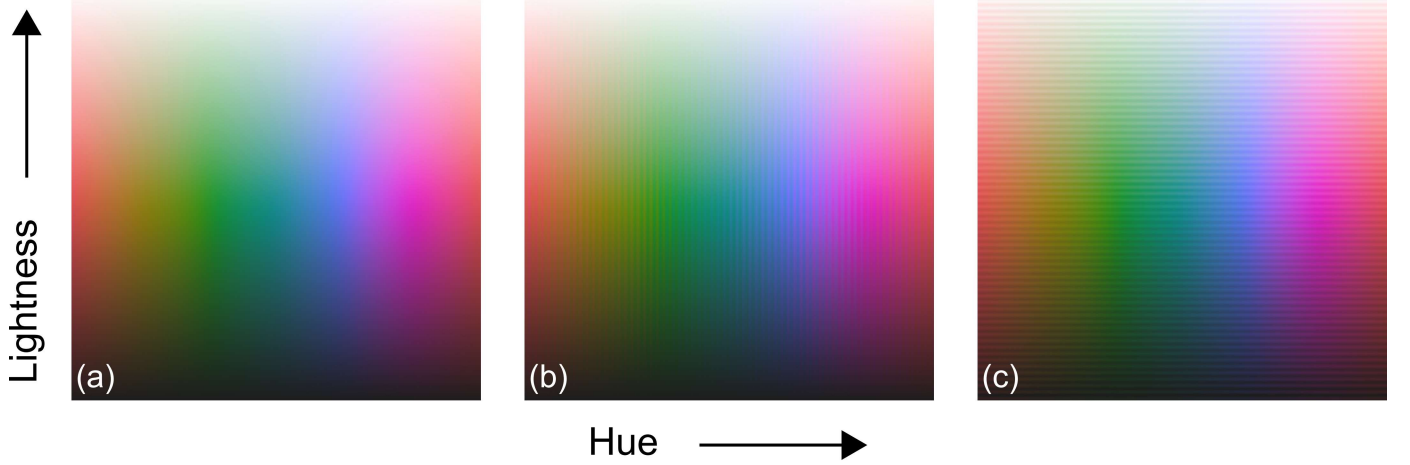


Fig. 3. A bi-cone in LUV space is free from visual discontinuities (a) but covers a limited gamut. The bicone has minimal hue contrast (b, horizontal sinusoidal ramp) since $\frac{\partial L^*}{\partial \text{hue}} = 0$, but excellent lightness contrast uniformity (c, vertical sinusoidal ramp).

$$\text{halves of space: } \int_{h^*, l^*=0}^{l^*=\frac{1}{2}} |\partial L^*| = \int_{h^*, l^*=\frac{1}{2}}^{l^*=1} |\partial L^*|$$

A bipyramid provides an excellent starting point to simultaneously satisfy these requirements. First, h^* is mapped to LUV space using fractional progress around the bipyramid equator. Next, l^* is incorporated by linear interpolation with the light or dark peak (for $l^* < \frac{1}{2}$ or $l^* > \frac{1}{2}$ respectively). Finally, chromaticity is scaled by s^* . Selecting alternating light and dark control points at $L^* = \bar{L}^* \pm \Delta L^*$ for the equator allows transfer of contrast from l^* to h^* . With this construction, the constraints can be satisfied with equatorial control points denoted p^i :

- 1) Grayscale when fully unsaturated: peaks at $(L^*, u^*, v^*) = (L_{\min/\max}^*, u^*, v^*)$
- 2) Grayscale at lightness endpoints: peaks at $(L^*, u^*, v^*) = (L_{\min/\max}^*, u^*, v^*)$
- 3) Maximum chromaticity at lightness midpoint: satisfied by construction
- 4) Free from visual discontinuities: not fully addressed (C^0 but not C^1)
- 5) Stay within the RGB gamut: bipyramid \subset RGB
- 6) Maximize gamut volume: minimize L_{\min}^* , maximize L_{\max}^* , maximize $c^*(p^i)$
- 7) Maximize hue contrast: maximize $|p^i - p^{i+1}|_{L^*}$
- 8) Maximize lightness contrast: maximize $|L_{\min/\max}^* - p^i|_{L^*}$
- 9) Maximize hue perceptual uniformity: even number of control points and maximize ΔL^*
- 10) Maximize lightness perceptual uniformity: minimize ΔL^*
- 11) Evenly distribute contrast between light and dark halves of space: $\bar{L}^* = \frac{L_{\min}^* + L_{\max}^*}{2}$

C^1 continuity with respect to h^* can be achieved by replacing the equator with a higher order spline. A cubic B-spline was chosen for this work since it is the lowest order satisfying C^1 continuity and with the B-spline closest to the first control point for $h^* = 0$ for an unclamped, uniform spline (odd order) [19]. Two extra points were linearly interpolated between neighboring control points to limit the influence of nonadjacent control points. A piece-

wise polynomial correction to the lightness enforces C^1 continuity of L^* with respect to l^* :

$$L_{C^1}^* = \begin{cases} c_1 \cdot l^* + d_1 : & l^* \leq \frac{1}{2} - t_l \\ a_2 \cdot l^{*3} + b_2 \cdot l^{*2} + c_2 \cdot l^* + d_2 : & \frac{1}{2} - t_l < l^* \leq \frac{1}{2} \\ a_3 \cdot l^{*3} + b_3 \cdot l^{*2} + c_3 \cdot l^* + d_3 : & \frac{1}{2} < l^* < \frac{1}{2} + t_l \\ c_4 \cdot l^* + d_4 : & \frac{1}{2} + t_l \leq l^* \end{cases} \quad (9)$$

C^1 continuity of c^* with respect to l^*

$$c_{C^1}^* = c^* * \begin{cases} x & : x \leq t_c \\ a \cdot x^3 + b \cdot x^2 + c \cdot x + d & : t_c < x \end{cases} \quad (10)$$

$$x = 2 \cdot \begin{cases} l^* & : l^* \leq \frac{1}{2} \\ 1 - l^* & : l^* > \frac{1}{2} \end{cases} \quad (11)$$

Independent corrections are applied instead of using a spline through the bipyramid tips and equator point to maintain as much contrast uniformity as possible. The 12 unknowns in equation 9 are solved for by enforcing C^2 continuity at the transitions and the values at l^* at 0, $\frac{1}{2}$, and 1 (L_{\min}^* , L_{equator}^* , and L_{\max}^* , respectively). The 4 unknowns in equation 10 are solved for by enforcing C^2 continuity at the transition and C^1 continuity across the equator ($\frac{\partial c^*}{\partial l^*}|_{l^*=\frac{1}{2}} = 0$). The adjustments to enforce continuity are shown schematically in figure 2.

Given the constraints and C^1 corrections, the following rules result in high quality HSL_U color spaces.

- 1) Select a minimal number of control points (4 or 6) since each additional point introduced a small perceptual flat spot to enforce C^1 continuity.
- 2) Select a widely spaced black and white point ($L_{\min/\max}^*$) with a midpoint near a luminance with wide RGB gamut chromaticity.
- 3) Select a luminance offset, ΔL^* , to balance h^* and l^* contrast ($\Delta L^* = \frac{L_{\max}^* - L_{\min}^*}{N_{\text{pts}}}$ distributes contrast

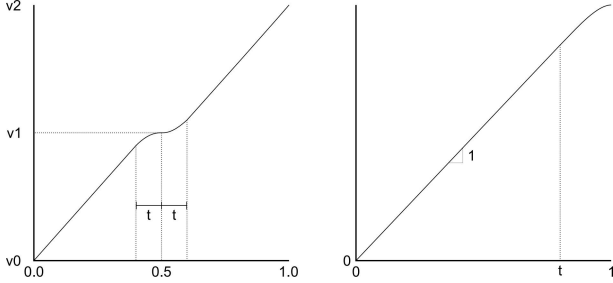


Fig. 4. The nonlinear adjustments required for lightness (left) and chromaticity (right) continuity are shown schematically.

- across h^* and l^* proportional to the solid angle covered).
- 4) Place control points on the surface of the RGB gamut at $L^* = \bar{L}^* \pm \Delta L^*$ at desired primary colors.
 - 5) Scale chromaticity of control points as needed if the RGB gamut is violated.

3 PERCEPTUALLY UNIFORM CYLINDRICAL COLOR SPACES

Using the above guidelines, two HSL_U spaces have been constructed with six and four control points, respectively. Both spaces use $L_{\min}^* = 12$ and $L_{\max}^* = 98$, a compromise between contrast and gamut maximization (the RGB gamut has limited chromaticity at $L^* = 50$ and none at $L^* = 100$). $\Delta L^* = 15$ was used for both maps, which distributes contrast evenly between h^* and l^* for six control points but favors lightness contrast for four control points ($\Delta L^* = 22.5$ severely limits chromaticity for dark points). The dark green control point was selected first for the 4 fold color space since green has limited chromaticity at $L^* = 40$. The most chromatic points at 90° intervals were selected for the remaining 3 control points. The most chromatic red, green, and blue colors in the RGB gamut at $L^* = 40$ were selected as the dark control points for the six fold color map. The light control points are the most chromatic points in the RGB gamut at the bisecting angles. The control point coordinates in LUV space are provided in table 3. The values 0.1 and 0.8 were selected empirically for the transition region parameters t_l and t_c in equations 9 and 10. Wider transition regions improve perceptual uniformity at the expense of contrast uniformity. The resulting color spaces are free from perceptual discontinuities and exhibit excellent perceptual uniformity as shown in figure 3. The gamuts of each space are shown in comparison to the standard RGB gamut in figure 3.

4 INVERSION SYMMETRY

Inversion symmetry on the bi-cone can be accomplished by restricting either hue or lightness to $[0, \frac{1}{2}]$ and doubling to recover $[0, 1]$ [13]. Doubling lightness creates a color degeneracy at $l^* = \frac{1}{2}$ with $HSL_U = (h^*, 1, \frac{1}{2})$ being white for all hues, but maintains perceptual uniformity of l^* at $l^* = \frac{1}{2}$. Since each map produces a double covering, the light or dark half of the bicone can be selected for a total of 4 inversion symmetry permutations shown in figure 4. Doubling hue does not introduce a degeneracy at $l^* = \frac{1}{2}$, but breaks

TABLE 1
Control point coordinates are provided for the six and four fold HSL_U spaces.

	L^*	u^*	v^*	swatch
six	40	131.5	28.4	■
	70	27.1	74.3	■
	40	-37.9	49.0	■
	70	-53.7	-15.0	■
	40	-15.2	-132.9	■
	70	68.7	-62.2	■
four	40	55.7	-72.1	■
	70	86.7	67.1	■
	40	-37.7	49.0	■
	70	-50.7	-39.2	■

C^1 continuity and introduces a noticeable artifact, as shown in figure 4. The artifact can be removed by modifying the nonlinear adjustment to be symmetric (i.e. $v0=v2$ in figure 2), but a perceptual flat spot is created instead since the lightness reversal introduces a local extremum, as shown in figure 4.

5 COLOR MAPS

Using HSL_U color spaces as a basis, perceptually uniform color maps for the disk and sphere are trivial:

$$(r, \theta)_w \mapsto (h^*, s^*, l^*) = \left(\frac{\theta}{2\pi} \bmod 1, 1, 1 - \frac{r}{2r_{\max}} \right) \quad (12)$$

$$(r, \theta)_k \mapsto (h^*, s^*, l^*) = \left(\frac{\theta}{2\pi} \bmod 1, 1, \frac{r}{2r_{\max}} \right) \quad (13)$$

$$(\theta, \phi) \mapsto (h^*, s^*, l^*) = \left(\frac{\theta}{2\pi} \bmod 1, 1, 1 - \frac{\phi}{\pi} \right) \quad (14)$$

Extension to the unit ball is possible by constructing concentric bicones, creating a color space that is perceptually uniform with respect to both hue and lightness for any given fractional radius r^* :

$$(h^*, r^*, l^*) \mapsto (L^*, u^*, v^*) = (\bar{L}^* + (\bar{L}^* - L^*)|_{(h^*, l^*)} \cdot r^*, u^*|_{(h^*, l^*)} \cdot r^*, v^*|_{(h^*, l^*)} \cdot r^*) \quad (15)$$

The resulting concentric surfaces are shown for a range of radii in figure 5. This mapping enables color maps for the ball that are perceptually uniform with respect to azimuthal and polar angle for any given radius and are free from visual discontinuities:

$$(r, \theta, \phi) \mapsto (h^*, r^*, l^*) = \left(\frac{\theta}{2\pi} \bmod 1, \frac{r}{r_{\max}}, 1 - \frac{\phi}{\pi} \right) \quad (16)$$

Sections of the resulting ball colormap with the test signal applied to each of the three components are shown in figures 5 and 5. The sections demonstrate that there is a perceptually flat direction at each point ($\partial L^* = 0$), but overall exhibit good perceptual uniformity. Some sections show no contrast because the perturbation is in the same direction locally, e.g. applying the test signal to the azimuthal angle when viewing a section orthogonal to the l^* axis (as in the center of figure 5) is equivalent to rotating the section, generating no ripple effect.

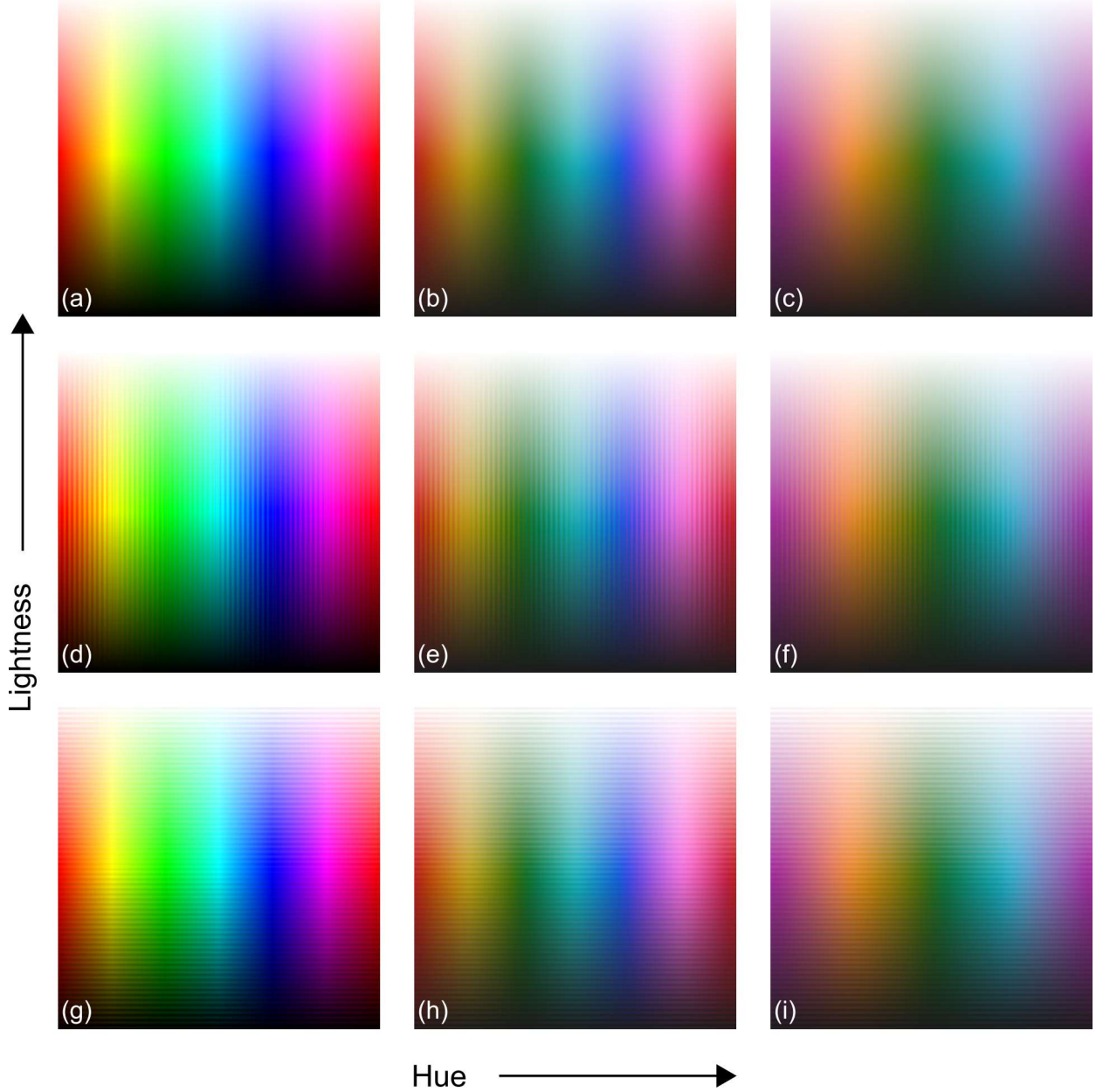


Fig. 5. The saturated surface of HSL space (a) has false features due to discontinuities in L^* gradients, but the surface of a uniform bi-cone with 6 control points (b) and 4 control points (c) is smooth. Application of a test signal to the hue (d) and lightness (g) components of HSL space reveals perceptual flat spots and non-uniform contrast in both. Coloring the same signal with a uniform bi-cone space show consistent hue (e,f) and lightness (h,i) contrast, but sacrifices accessible gamut.

5.1 Application

The in-plane magnetization component of a micromagnetics simulation is shown with 3 color maps in figure 5.1 [1], [20]. The data is colored using the maps in equations 4 and 13 with both the four and six control point HSL_U spaces used. In addition to perceptual non-uniformity, HSV coloring of the vector field over-emphasizes green directions and under-emphasizes blue directions. Additionally, fractional angles devoted to each color are uneven with red, green, and blue being over-represented. HSL_U coloring of the vector field equally emphasizes all primary colors, evenly distributes fractional angles to each color, and provides perceptually uniform contrast with respect to direction and magnitude. Six control point coloring offers a similar aes-

thetic to HSV coloring while four control point coloring is more suitable for identifying compass directions.

In texture analysis, perceptually uniform IPF colors are possible by first mapping the fundamental sector to the hemisphere using the method of Nolze et al [13]. This method has C^1 discontinuities at the directions corresponding to the corners of the fundamental sector, leading to visual discontinuities. C^1 continuity can be enforced by filleting the corners with a 3rd degree polynomial, similar to the HSL_U construction, as shown in figure 5.1. The filleting introduces a small perceptual flat spot at each corner, providing a trade off between perceptually uniform area and visual discontinuities. A truly conformal mapping, e.g. Schwarz-Christoffel, may produce a more optimal balance

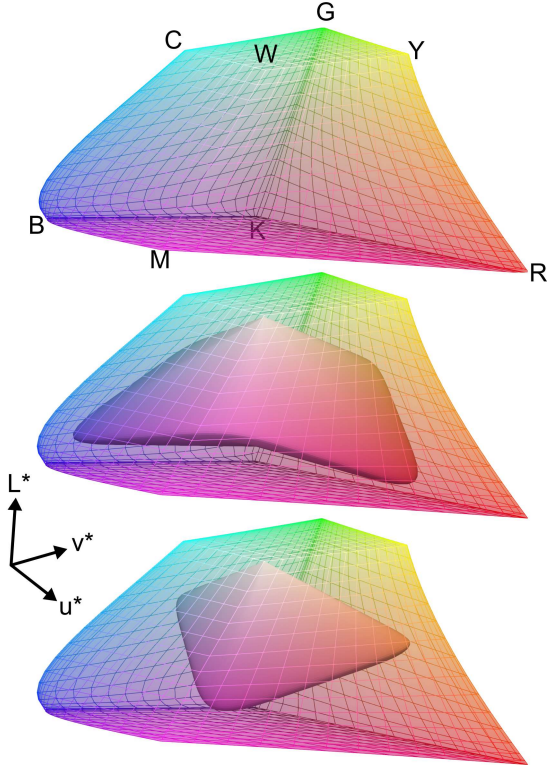


Fig. 6. The standard RGB gamut is shown with corners of the RGB cube indicated (top). The gamuts of the 6 (center) and 4 (bottom) control point HSL_U spaces are shown within the RGB gamut.

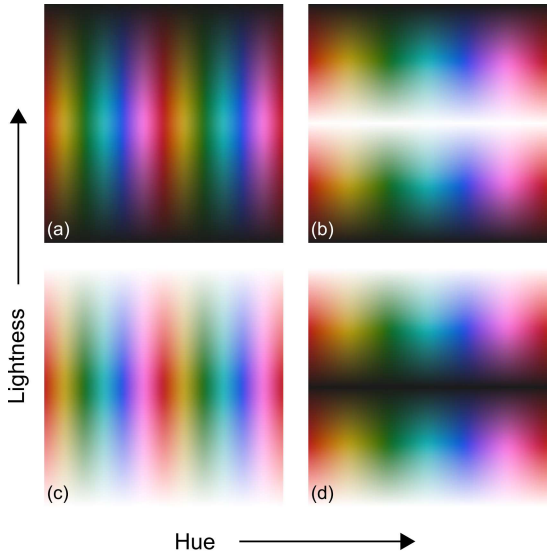


Fig. 7. The double covering from introducing inversion symmetry to bi-cone spaces enables two configurations for doubling hue (left) and lightness (right) for a total of four combinations. Black poles are the default (top) since $l^* = 0$ is black and white poles (bottom) are constructed by subtracting l^* from 1.

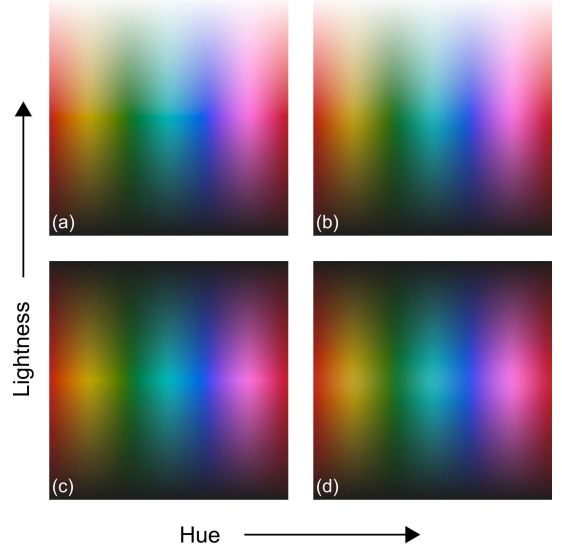


Fig. 8. A slight visual discontinuity is visible at $l^* = \frac{1}{2}$ if only C^0 continuity is enforced (a). Enforcing C^1 continuity removes the artifact (b). Adding a mirror plane breaks C^1 continuity and introduces a larger visual discontinuity due to the large gradient discontinuity (c). Enforcing C^1 continuity with the mirror plane removes the discontinuity (d).

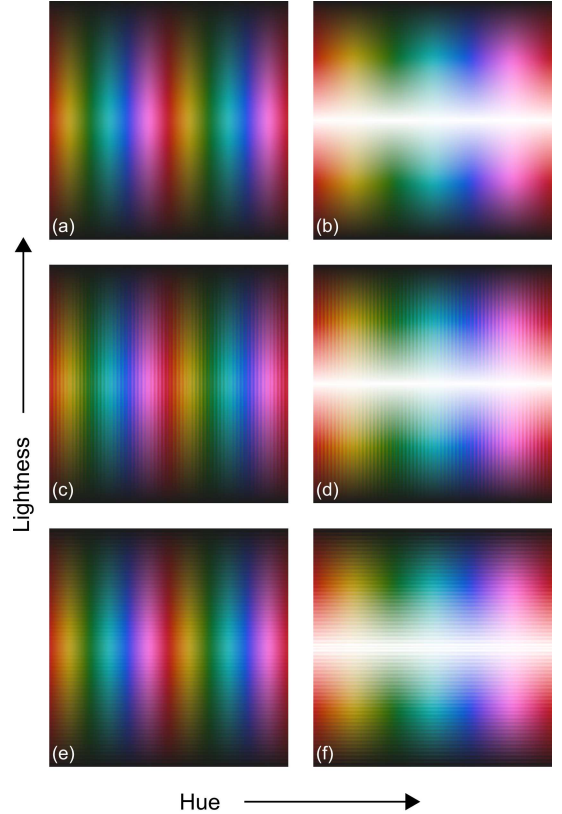


Fig. 9. Uniform bi-cone spaces can be given inversion symmetry by doubling either hue (a) or lightness (b). Doubling hue maintains uniform hue contrast (c), but enforcing C^1 continuity creates a perceptual flat spot in lightness contrast (e). Double lightness creates a perceptual flat spot in hue due to the degeneracy at $l^* = \frac{1}{2}$ (d), but has uniform lightness contrast (f).

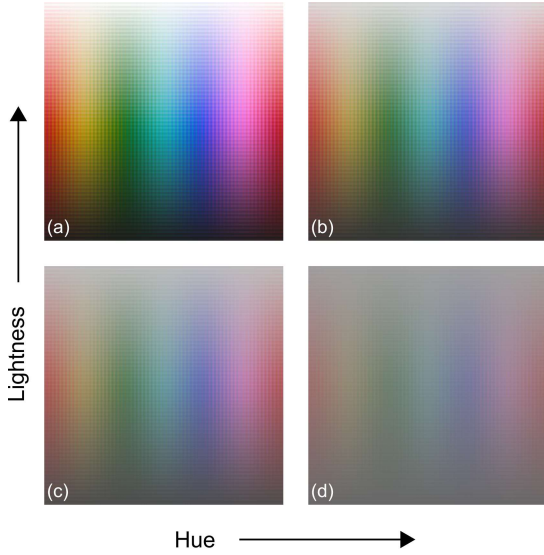


Fig. 10. Concentric bicones allow addition of a radial parameter that scales distance from the bicone center. Isosurfaces are shown for radii of 1 (a), $\frac{3}{4}$ (b), $\frac{1}{2}$ (c), and $\frac{1}{4}$ (d) with the test signal applied to both hue and lightness. The isosurface for 0 is solid gray ($L^* = 55$).

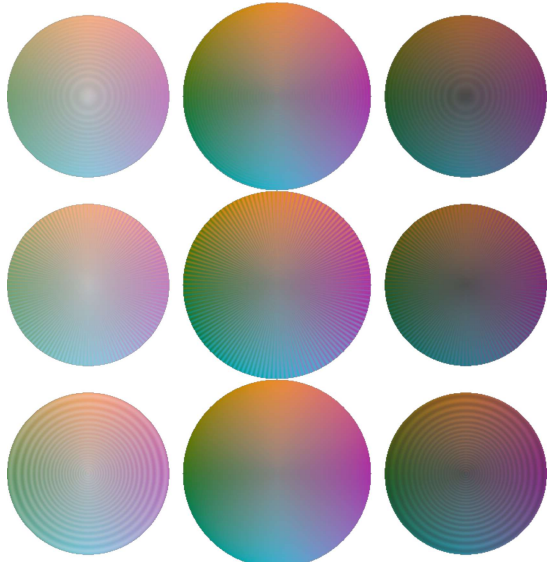


Fig. 11. Sections of the four fold ball color map are shown for $l^* = \frac{3}{4}$ (left), $l^* = \frac{1}{2}$ (center), and $l^* = \frac{1}{4}$ (right) with the test signal applied to radius (top), azimuthal angle (center), and polar angle (bottom).

in exchange for larger perturbations to uniformity and increased computational cost [21]. A cutoff distance of 0.05 times the angle between adjacent corners was empirically selected to balance softening of the discontinuity with the area of the flat regions.

The resulting hemisphere mapping produces a perceptually uniform IPF triangle that is free from discontinuities (both within the triangle and across mirror planes). A comparison of a simple HSV based IPF triangle, the IPF coloring of Nolze et al. and the HSL_U based triangle is shown in figure 5.1. For comparison, the IPF coloring is applied to a highly deformed dataset [22] shown in figure 5.1, demonstrating the improved capacity to visualize orientation gradients.

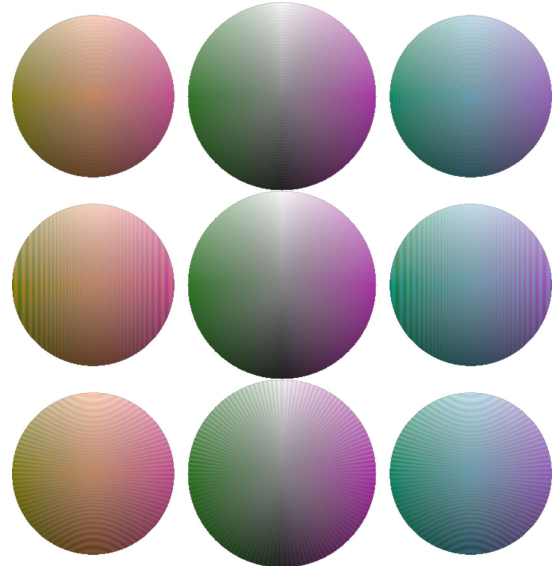


Fig. 12. Sections of the four fold unit ball color map are shown for $y = \frac{3}{4}$ (left), $y = \frac{1}{2}$ (center), and $y = \frac{1}{4}$ (right) with the test signal applied to radius (top), azimuthal angle (center), and polar angle (bottom).

6 SUMMARY

A framework for construction of perceptually uniform HSL like spaces was developed. HSL_U spaces are free from visual discontinuities and have uniform perceptual contrast with respect to hue and lightness. Procedures for introducing inversion symmetry without disrupting perceptual continuity or visual artifacts were developed. HSL_U spaces suitable for 4 and 6 fold symmetry were constructed and serve as the basis for perceptually uniform pseudocolor maps for the unit disk, unit sphere, and unit ball. A C^1 continuous mapping from a spherical triangle to the hemisphere allows generation of perceptually uniform IPF colors. Example applications of HSL_U based maps demonstrate perceptual uniformity and enable improved data visualization. An open source, C++ library for HSL_U color spaces with Python bindings is available at www.github.com/wlenthe/uniformbiconge.

ACKNOWLEDGMENTS

WL and MDG would like to acknowledge a DoD Vannevar-Bush Faculty Fellowship (# N00014-16-1-2821). All authors wish to acknowledge the computational facilities of the Materials Characterization Facility at CMU under grant # MCF-677785.

REFERENCES

- [1] A. Vansteenkiste, J. Leliaert, M. Dvornik, M. Helsen, F. Garcia-Sanchez, and B. Van Waeyenberge, "The design and verification of mumax3," *AIP advances*, vol. 4, no. 10, p. 107133, 2014.
- [2] R. Heilbronner and R. Kilian, "The grain size (s) of black hills quartzite deformed in the dislocation creep regime." *Solid Earth*, vol. 8, no. 6, 2017.
- [3] S. Peetersmans, M. Bopp, P. Vontobel, and E. Lehmann, "Energy-selective neutron imaging for three-dimensional non-destructive probing of crystalline structures," *Physics Procedia*, vol. 69, pp. 189–197, 2015. [Online]. Available: <http://www.sciencedirect.com/science/article/pii/S1875389215006379>

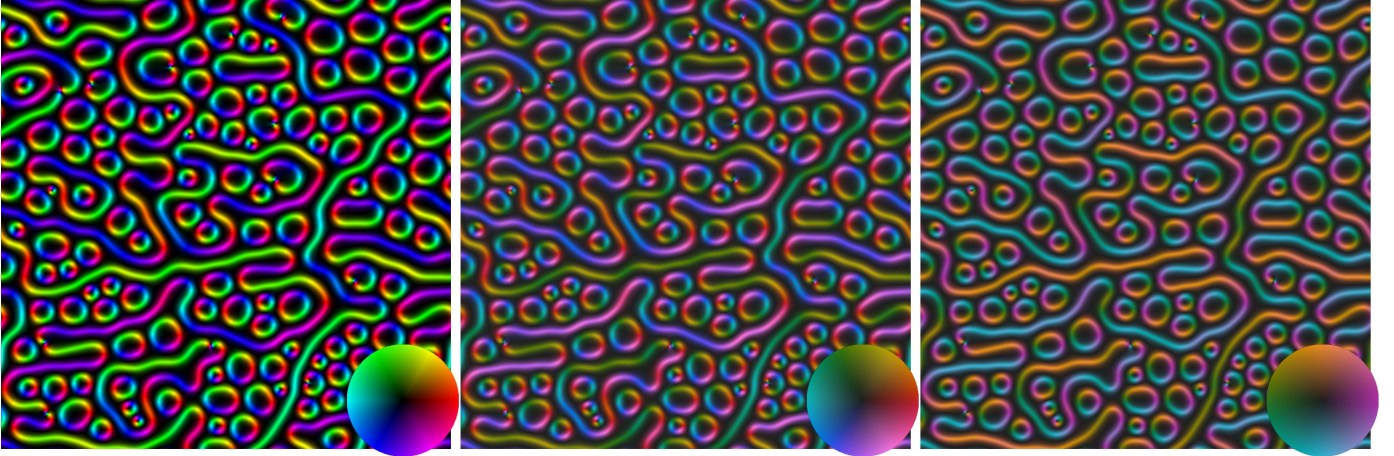


Fig. 13. The in-plane magnitude and direction of the magnetic field from a micromagnetics simulation colored with traditional HSL has non-uniform perceptual contrast (left). Additionally the large differences in relative intensities over-emphasize green directions and under-emphasize blue directions. Coloring the same data with six fold HSL_U (center) results in a similar aesthetic with perceptual uniformity. Coloring the same data with four fold HSL_U (right) is more appropriate when the four compass directions are the primary interest.

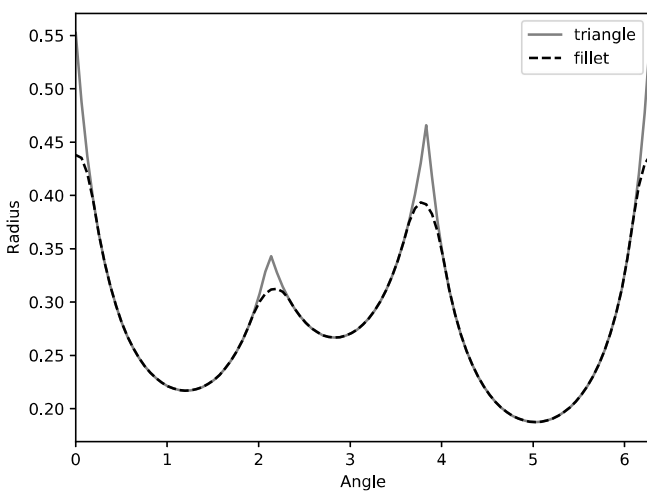


Fig. 14. Plotting maximum radius against angle for the cubic IPF triangle (solid gray) reveals discontinuities at triangle corners, resulting in visual discontinuities when colored. Smoothing the transition regions with a cubic polynomial (dashed black) enforces C^1 continuity.

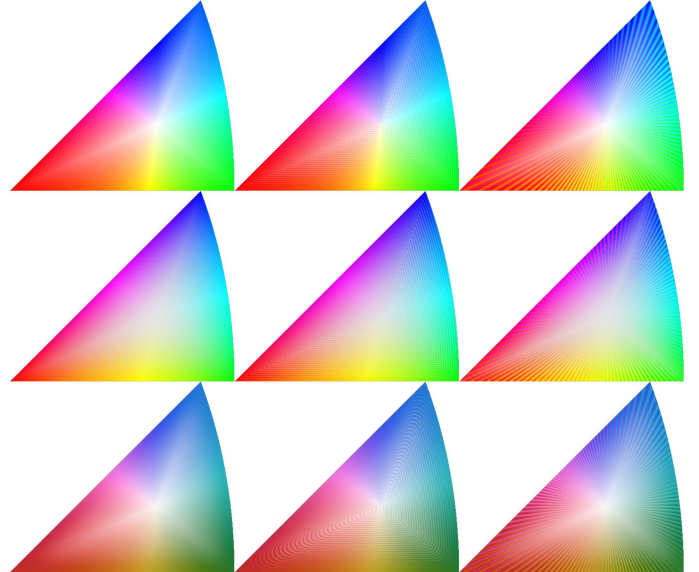


Fig. 15. Simply mapping the fundamental triangle to HSL or HSV space using the method of Nolze et al. introduces new discontinuities near the corners due to the first order discontinuity in radius (top) [13]. Applying the nonlinear hue and lightness corrections of Nolze et al. softens the discontinuities (middle) but retains the perceptual nonuniformity. Enforcing C^1 continuity in radius and using HSL_U space results in a perceptually uniform map free from discontinuities with small flat spots near the corners (bottom).

- [4] P. Kovesi, "Good colour maps: How to design them," *arXiv preprint arXiv:1509.03700*, 2015.
- [5] D. Borland and R. M. T. Ii, "Rainbow color map (still) considered harmful," *IEEE computer graphics and applications*, vol. 27, no. 2, 2007.
- [6] B. E. Rogowitz, L. A. Treinish, and S. Bryson, "How not to lie with visualization," *Computers in Physics*, vol. 10, no. 3, pp. 268–273, 1996.
- [7] C. Ware, "Color sequences for univariate maps: Theory, experiments and principles," *IEEE Computer Graphics and Applications*, vol. 8, no. 5, pp. 41–49, 1988.
- [8] G. H. Joblove and D. Greenberg, "Color spaces for computer graphics," *SIGGRAPH Comput. Graph.*, vol. 12, no. 3, pp. 20–25, Aug. 1978. [Online]. Available: <http://doi.acm.org/10.1145/965139.807362>
- [9] C. A. Schneider, W. S. Rasband, and K. W. Eliceiri, "Nih image to imagej: 25 years of image analysis," *Nature methods*, vol. 9, no. 7, p. 671, 2012.
- [10] U. Ayachit, *The ParaView Guide: A Parallel Visualization Application*. USA: Kitware, Inc., 2015.
- [11] M. Tkalcic and J. F. Tasic, "Colour spaces: perceptual, historical and applicational background," in *The IEEE Region 8 EUROCON 2003. Computer as a Tool.*, vol. 1, Sept 2003, pp. 304–308 vol.1.
- [12] M. D. Fairchild, *Color appearance models*. John Wiley & Sons, 2013.
- [13] G. Nolze and R. Hielscher, "Orientations-perfectly colored," *Journal of Applied Crystallography*, vol. 49, no. 5, pp. 1786–1802, 2016.
- [14] G. Booth, H. Zollinger, K. McLaren, W. G. Sharples, and A. Westwell, "Dyes, general survey," *Ullmann's Encyclopedia of Industrial Chemistry*, 2000.
- [15] P. Robertson and J. O'Callaghan, "The generation of color sequences for univariate and bivariate mapping," *IEEE Comput. Graph. Appl.*, vol. 6, no. 2, pp. 24–32, Feb. 1986. [Online]. Available: <http://dx.doi.org/10.1109/MCG.1986.276688>
- [16] C. Ware, "Quantitative texton sequences for legible bivariate maps," *IEEE Transactions on Visualization and Computer Graphics*, vol. 15, no. 6, 2009.

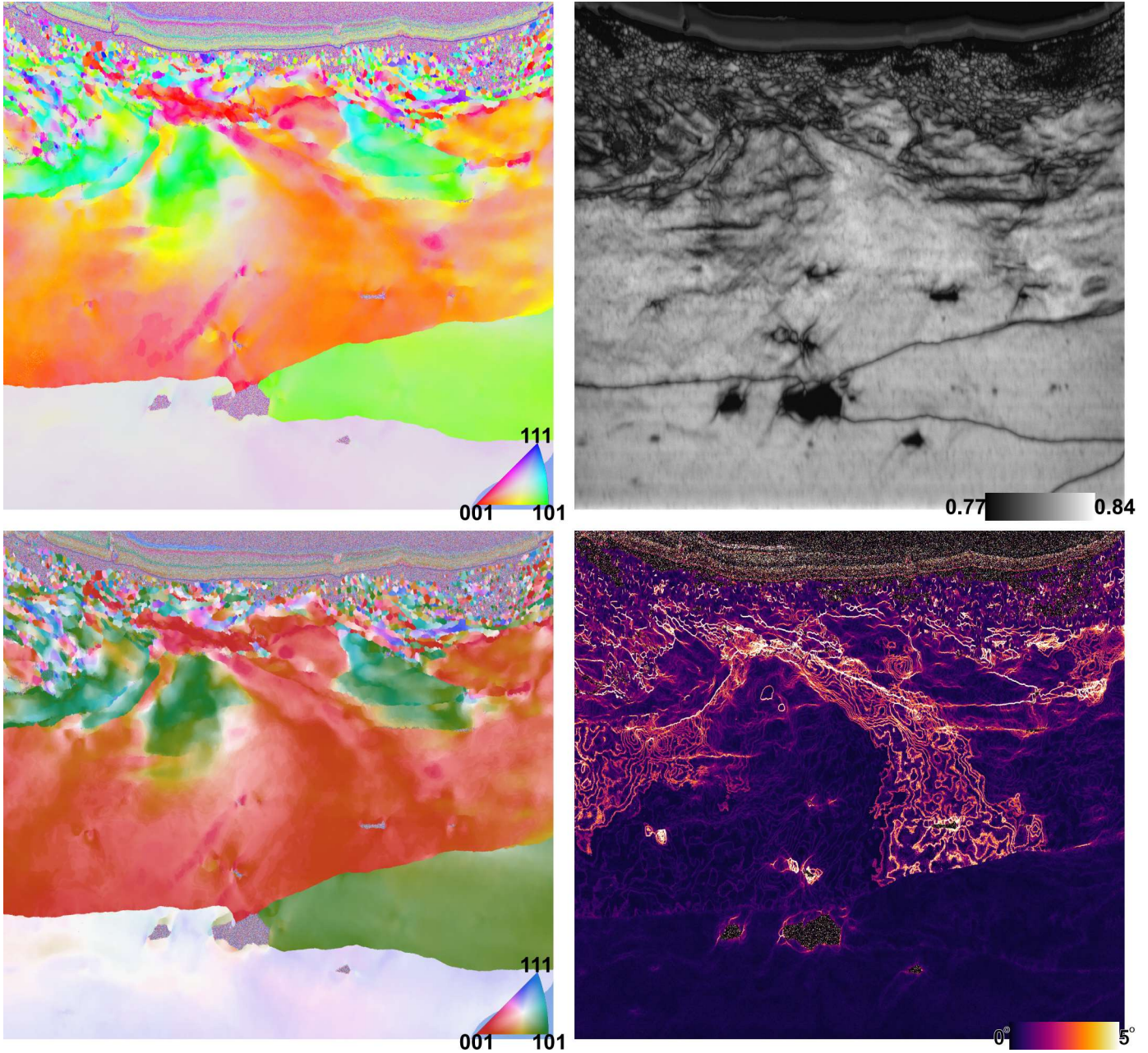


Fig. 16. A dictionary indexed shot peened aluminum sample is colored using the IPF method of Nolze et al. (top left) and maximum dot product (top right) [13], [22]. Coloring the same dataset with perceptually uniform IPF colors (bottom left) results in uniform contrast more closely aligned with kernel average misorientation (bottom right).

- [17] J. N. Kather, C.-A. Weis, A. Marx, A. K. Schuster, L. R. Schad, and F. G. Zöllner, "New colors for histology: optimized bivariate color maps increase perceptual contrast in histological images," *PLoS one*, vol. 10, no. 12, p. e0145572, 2015.
- [18] B. Pham, "Spline-based color sequences for univariate, bivariate and trivariate mapping," in *Visualization, 1990. Visualization'90., Proceedings of the First IEEE Conference on*. IEEE, 1990, pp. 202–208.
- [19] C. De Boor, C. De Boor, E.-U. Mathématicien, C. De Boor, and C. De Boor, *A practical guide to splines*. Springer-Verlag New York, 1978, vol. 27.
- [20] M. P. Li, M. De Graef, and V. Sokalski, "Lorentz tem image simulations of dzyaloshinskii domain walls under an in-plane magnetic field," *Microscopy and Microanalysis*, vol. 23, no. S1, pp. 1734–1735, 2017.
- [21] L. N. Trefethen, "Numerical computation of the schwarz-christoffel transformation," *SIAM Journal on Scientific and Statistical Computing*, vol. 1, no. 1, pp. 82–102, 1980.
- [22] S. Singh, Y. Guo, B. Winiarski, T. Burnett, P. Withers, and M. De Graef, "High resolution low kv EBSD of heavily deformed and nanocrystalline Aluminium by dictionary-based indexing," *Nature Scientific Reports*, vol. 8, p. 10991, 2018.